
SUBOPTIMAL SHAPLEY VALUE EXPLANATIONS

Xiaolei Lu

xiaoleilu2-c@my.cityu.edu.hk

ABSTRACT

Deep Neural Networks (DNNs) have demonstrated strong capacity in supporting a wide variety of applications. Shapley value has emerged as a prominent tool to analyze feature importance to help people understand the inference process of deep neural models. Computing Shapley value function requires choosing a baseline to represent feature’s missingness. However, existing random and conditional baselines could negatively influence the explanation. In this paper, by analyzing the suboptimality of different baselines, we identify the problematic baseline where the asymmetric interaction between x'_i (the replacement of the faithful influential feature) and other features has significant directional bias toward the model’s output, and conclude that $p(y|x'_i) = p(y)$ potentially minimizes the asymmetric interaction involving x'_i . We further generalize the uninformativeness of x'_i toward the label space L to avoid estimating $p(y)$ and design a simple uncertainty-based reweighting mechanism to accelerate the computation process. We conduct experiments on various NLP tasks and our quantitative analysis demonstrates the effectiveness of the proposed uncertainty-based reweighting mechanism. Furthermore, by measuring the consistency of explanations generated by explainable methods and human, we highlight the disparity between model inference and human understanding.

1 Introduction

Nowadays Deep Neural Networks (DNNs) have demonstrated impressive results on a range of tasks. For example, Language Models Devlin et al. [2018], Chowdhery et al. [2022], Thoppilan et al. [2022], OpenAI [2023] show strong capacity in the field of Natural Language Processing (NLP), Computer Vision (CV) and speech processing. Unlike traditional models (e.g. conditional random fields) that optimize weights on human interpretable features, deep neural models operate like black-box models by applying multiple layers of non-linear transformation on the vector representations of input data, which fails to provide insights to understand the inference process of deep neural models.

Feature attribution methods Kim et al. [2018] identify how much each feature contribute to the model’s output, which could indicate how a deep model make decisions. Shapley value Shapley et al. [1953], measuring the marginal contribution that a player makes upon joining the group by averaging over all possible permutations of players in the group, has been the prominent feature attribution to analyze feature importance toward model’s output. For example, SHAP Lundberg and Lee [2017], L-Shapley Chen et al. [2018] and WeightedSHAP Kwon and Zou [2022].

Computing Shapley value function requires choosing a baseline to represent feature’s missingness. The most common solution is to fill in the missingness by randomly sampling from the dataset Štrumbelj and Kononenko [2014]. Another way is to generate features by conditioning on the observed features to replace the missing parts. However, Frye et al. [2020] and Hooker et al. [2021] argue that random sampling operation ignores inherent feature dependency. Also, it is difficult for conditional sampling based Shapley value to distinguish correlated feature with different sensitivity toward the model’s output Janzing et al. [2020], Kumar et al. [2020]. Watson [2022] considered the baselines sampled from interventional distribution is optimal but it requires accessing to the underlying causal structure.

In this paper, we study the faithfulness of Shapley-based model interpretation. Our contributions are summarized as follows:

- We analyze the suboptimality of different baselines for computing Shapley value in interpreting feature importance, and introduce asymmetric interaction to identify the problematic baseline where the interaction between x'_i (the replacement of the faithful influential feature) and other features has significant directional bias toward the model’s output.

- We propose that $p(y|\mathbf{x}'_i) = p(y)$ potentially minimizes the asymmetric interaction involving \mathbf{x}'_i . By generalizing the unformativeness of \mathbf{x}'_i toward the label space L to avoid estimating $p(y)$, we design a simple uncertainty-based reweighting mechanism to accelerate the computation process.
- We conduct quantitative analysis on various tasks to demonstrate the faithfulness of the proposed uncertainty-based reweighting mechanism, and measure the consistency of explanations generated by explainable methods and human to highlight the disparity between model inference and human understanding.

2 Related work

2.1 Interpretability of deep models

Different from white-box models (e.g. decision tree-based models) that are intrinsically interpretable, deep models operate like black-box models where the internal working mechanism are not easily understood. Existing methods for interpreting deep models could be categorized into two types: feature attribution that focuses on understanding how a fixed black-box model leads to a particular prediction, and instance attribution is to trace back to training data and study how a training point influence the prediction of a given instance. For example, Integrated Gradients Sundararajan et al. [2017] measures feature importance by computing the path integral of the gradients respect to each dimension of input. LIME Ribeiro et al. [2016] generates explanation by learning an inherently interpretable model locally on the instance being explained. Shapley value Shapley et al. [1953] that is derived from cooperative game theory treats each feature as a player and computes the marginal contribution of each feature toward the model’s output. Regarding instance attribution, typical methods include influence function Koh and Liang [2017] which attends to the final iteration of the training and TracIn Pruthi et al. [2020] that keeps tracing the whole training process.

2.2 Shapley value

Lloyd Shapley’s idea Shapley et al. [1953] is that players in the game should receive payments or shares proportional to their marginal contributions. Štrumbelj and Kononenko [2014] and Lundberg and Lee [2017] generalize Shapley value to measure feature importance toward the model’s output by averaging marginal contribution of the feature being explained over all possible permutations among features. There are many variants of Shapley value to address efficiency and faithfulness. For example, to improve efficiency of Shapley value, Chen et al. [2018] proposes L-Shapley to explore local permutations and C-Shapley to compute valid connected nodes for structured data. Kwon and Zou [2022] proposes WeightedSHAP to optimize weight of each marginal contribution under the user-defined utility function to emphasize influential features.

Computing Shapley value function requires choosing a baseline to represent feature’s missingness. Random baseline Lundberg and Lee [2017], Chen et al. [2018], Kwon and Zou [2022] has been widely used due to its immediate availability. Since random baseline ignores inherent feature dependency and thus could result in inconsistent context, Frye et al. [2020] and Hooker et al. [2021] address the importance of conditional baseline where the missingness is replaced with the features generated by conditioning on the observed features. However, Janzing et al. [2020] and Kumar et al. [2020] use simple linear model to demonstrate that conditional baseline based Shapley value fails to distinguish correlated feature with different sensitivity toward the model’s output. Watson [2022] considers that the optimal baseline should follow the interventional distribution but it requires accessing to the underlying causal structure. Generally for the above baselines none is more broadly applicable than the others, which motivates us to analyze suboptimality of these baselines for Shapley value on interpreting black-box models and find out the optimal baseline.

3 Suboptimal baselines for Shapley value toward black-box model interpretation

3.1 Preliminaries

In supervised setting, given an input $\mathbf{x} = (\mathbf{x}_1, \dots, \mathbf{x}_n)$ and a prediction model f , let $f_y(\cdot)$ denotes the model output probability on y , the Shapley value of i_{th} feature in \mathbf{x} for the model prediction y is weighted and summed over all possible feature combinations as

$$\phi(i) = \sum_{S \subseteq n \setminus i} \frac{(n-1-|S|)!|S|!}{n!} [v(S \cup i) - v(S)], \quad (1)$$

where S is the subset of feature indices. $v(S)$ is the value function that measures the change in prediction caused by observing certain subsets S in the instance Štrumbelj and Kononenko [2014] and is defined as

$$v(S) = \mathbb{E}(f_y|\mathbf{x}_S \cup \mathbf{x}'_{\bar{S}}) - \mathbb{E}(f_y|\mathbf{x}'), \quad (2)$$

where \mathbf{x}' collectively denotes all possible instances and $\mathbb{E}(f_y|\mathbf{x}')$ represents the model’s prediction averaged across these instances (this item could be excluded when computing the difference between $v(S \cup i) - v(S)$). $\mathbf{x}_S \cup \mathbf{x}'_{\bar{S}}$ refers to the instances that retain unchanged subset values \mathbf{x}_S . The contribution of the subset S is determined by the difference between the effect of the subset S and the average effect.

There are three common baselines Watson [2022] to fill in $\mathbf{x}'_{\bar{S}}$ that are described below.

Random baseline: $\mathbf{x}'_{\bar{S}}$ is drawn randomly from the distribution $p(\mathbf{x}'_{\bar{S}})$.

Conditional baseline: sample $\mathbf{x}'_{\bar{S}}$ by conditioning on \mathbf{x}_S .

Interventional baseline: $\mathbf{x}'_{\bar{S}}$ is generated by following the causal data structure $p(\mathbf{x}'_{\bar{S}}|do(\mathbf{x}_S))$. Since accessing causal data structure is challenging we focus on discussing the above two baselines in this work.

3.2 A motivation example

It could be trivial to show how the random and conditional baselines lead to incorrect interpretation on white-box models (analysis of a linear model is described in Appendix A). In interpreting deep models with Shapley value, we analyze an empirical example with a movie review “*plot is fun but confusing*” that is predicted as “Negative” sentiment by our finetuned BERT classification model¹, the faithful feature contribution ranking² is [“*confusing*”, “*plot*”, “*but*”, “*is*”, “*fun*”]. Fig.1 shows the ranking of Shapley values computed by the random and conditional baselines with different number of sampling instances.

Random baseline: As shown in Fig.1a, by increasing the number of sampling instances, “*confusing*” and “*fun*” are always identified as the most influential features while the ranks of “*plot*” and “*but*” are misleading in most cases.

Conditional baseline: With smaller sampling size (i.e. [1, 20]) that could ensure feature consistency via conditional sampling, we observe that in these scenarios “*confusing*” and “*fun*” are the most influential features but the contribution of “*plot*” and “*but*” could be misinterpreted.

Given a fixed subset S , the contribution of i_{th} feature is computed with

$$\begin{aligned} \phi_S(i) &= v(S \cup i) - v(S) \\ &= \mathbb{E}(f_y|\mathbf{x}_{S \cup i} \cup \mathbf{x}'_{\bar{S}_1}) - \mathbb{E}(f_y|\mathbf{x}_S \cup \mathbf{x}'_{\bar{S}_2}), \end{aligned} \quad (3)$$

where $\bar{S}_1 \subseteq n \setminus (S \cup i)$ and $\bar{S}_2 \subseteq n \setminus S$.

For positively-contributing features, it is expected that without its participation $\mathbb{E}(f_y|\mathbf{x}_S \cup \mathbf{x}'_{\bar{S}_2})$ should be lower than $\mathbb{E}(f_y|\mathbf{x}_{S \cup i} \cup \mathbf{x}'_{\bar{S}_1})$. However, for highly influential positive features, under some random and conditional baselines $f_y(S \cup i)$ could be much lower than $f(S)$, which may results in lower $\phi_S(i)$ compared to less influential positive features. Similarly $\phi_S(i)$ for a highly influential negative feature could be higher than that of less influential negative features.

Taking $\mathbf{x}_i = \text{“plot”}$ with $\mathbf{x}_S = \text{“is fun but”}$ as an example (more baselines with random sampling and conditional sampling are shown in Appendix C). With conditional sampling, $f_y(\text{“practice is fun but brief”}) = 0.5147$ is much higher than $f_y(\text{“plot is fun but brief”}) = 0.0347$ and $f_y(\text{“script is fun but vague”}) = 0.8203$ exceeds $f_y(\text{“plot is fun but vague”}) = 0.7113$. Obviously, compared with “*plot*”, “*practice*” and “*script*” contribute more positively to y .

3.3 Error analysis: asymmetric feature interaction view

As described in Eq.(1), $\phi(\mathbf{x}_i)$ represents the average sum of the interactions between \mathbf{x}_i and all possible subsets of \mathbf{x} as

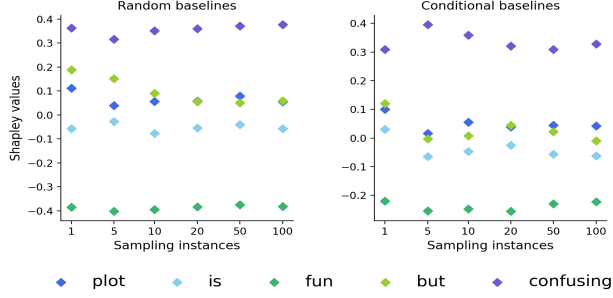
$$\phi(\mathbf{x}_i) = \sum_{\mathbf{S}(\mathbf{x}_i) \subseteq \mathbf{x}} \mathcal{I}(\mathbf{S}(\mathbf{x}_i)), \quad (4)$$

where $\mathcal{I}(\mathbf{S}(\mathbf{x}_i))$ denotes the interaction within the subset \mathbf{S} involving \mathbf{x}_i .

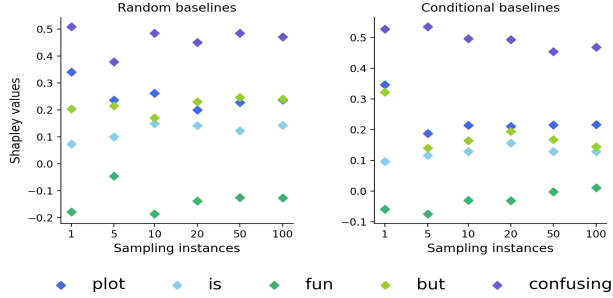
Existing feature interaction attribution methods assume symmetric interaction where each feature contributes equally to the interaction score, which fails to capture imbalanced relationship across features toward model predictions. For

¹The finetuned version is designed to predict this review as “Negative” that is consistent with the ground-truth.

²The faithful ranking is obtained by conducting quantitative analysis in Experimental section on the possible rankings provided by NLP researchers.

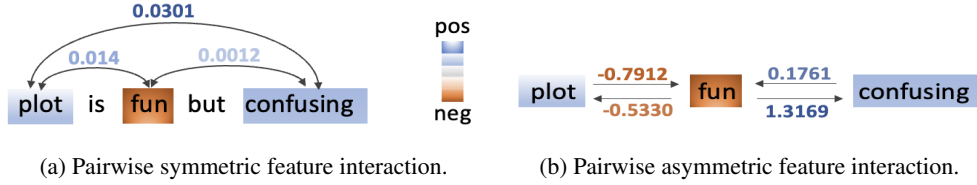


(a) The ranking of Shapley values computed without the uncertainty-based reweighting mechanism.



(b) The ranking of Shapley values computed with the uncertainty-based reweighting mechanism.

Figure 1: Comparison of the ranking of Shapley values without and with the uncertainty-based reweighting mechanism under different number of sampling instances. Sampling instances refer to the sampling size for computing $v(S)$.



(a) Pairwise symmetric feature interaction.

(b) Pairwise asymmetric feature interaction.

Figure 2: Demonstrations of our defined asymmetric feature interaction and the symmetric feature interaction computed by the Shapley interaction index.

example, as shown in Fig.2a, we present pairwise interactions computed by Shapley interaction index³ Grabisch [1997] among {"plot", "fun", "confusing"}. For positive influential "confusing", interacting with either negative or positive features leads to a positive impact on the predicted outcome y , indicating that influence of "confusing" can play a dominant role in some interactions.

To further explore and quantify the variable influence of x_i within these interactions, we introduce the concept of asymmetric interaction.

Asymmetric interaction. In the presence of the subset x_{T_2} , the asymmetric interaction between two subsets x_{T_1} and x_{T_2} toward the predicted outcome y is defined as

$$\phi(T_2 \rightarrow T_1) = C_1 \sum_{T_2 \subseteq S \subseteq n \setminus \{T_1\}} \Delta(T_2, T_1, \mathbf{x}) - C_2 \sum_{\substack{S_1, S_2 \subseteq n \setminus \{T_2\} \\ S_1 \cap S_2 = \emptyset}} \Delta(T_2, S_2, \mathbf{x}), \quad (5)$$

$$\Delta(T_2, T_1, \mathbf{x}) = I(y; \mathbf{x}_{T_1} | \mathbf{x}_S) - I(y; \mathbf{x}_{T_1} | \mathbf{x}_{S \setminus T_2}), \quad (6)$$

$$\Delta(T_2, S_2, \mathbf{x}) = I(y; \mathbf{x}_{T_2} | \mathbf{x}_{S_1 \cup S_2}) - I(y; \mathbf{x}_{T_2} | \mathbf{x}_{S_1}), \quad (7)$$

³We employ random sampling with larger sampling size to approximate the faithful interactions, and the computed value may not be faithful due to inherent suboptimality.

where $C_1 = \frac{1}{2^{n-|T_1|-|T_2|}}$ and $C_2 = \frac{1}{3^{n-|T_2|-2^{n-|T_2|+1+1}}}$ are the normalization terms. $I(\cdot)$ denotes the pointwise mutual information as

$$I(y; \mathbf{x}|\mathbf{x}') = \log \frac{p(y; \mathbf{x}|\mathbf{x}')}{p(y|\mathbf{x}')p(\mathbf{x}|\mathbf{x}')}. \quad (8)$$

$I(y; \mathbf{x}|\mathbf{x}')$ measures the amount of information that \mathbf{x} contributes to y when we already know \mathbf{x}' . $I(y; \mathbf{x}_{T_1}|\mathbf{x}_S) - I(y; \mathbf{x}_{T_1}|\mathbf{x}_{S \setminus T_2})$ quantifies the contribution of \mathbf{x}_{T_1} toward y in the presence of \mathbf{x}_{T_2} . Similarly, $I(y; \mathbf{x}_{T_2}|\mathbf{x}_{S_1} \cup \mathbf{x}_{S_2}) - I(y; \mathbf{x}_{T_2}|\mathbf{x}_{S_1})$ measures the influence between \mathbf{x}_{T_2} and \mathbf{x}_{S_2} on y . Asymmetric interaction $\mathbf{x}_{T_2} \rightarrow \mathbf{x}_{T_1}$ is quantified by computing the difference between average interaction contribution involving \mathbf{x}_{T_1} and \mathbf{x}_{T_2} , and the average interaction with \mathbf{x}_{T_2} . Fig.2b demonstrates pairwise asymmetric interactions among {"plot", "fun"} and {"fun", "confusing"}. We can observe that in the presence of different features, the corresponding interactions with "fun" could have directional contribution toward the predicted outcome y .

Feature influence. Given the asymmetric interaction graph $IG = (\mathbf{x}, \mathbf{E})$ where \mathbf{x} is the set of features in a given instance and \mathbf{E} is the set of all asymmetric interaction edges. Each asymmetric interaction edge is denoted as $e = (e_{\text{tail}}, e_{\text{head}})$. $\text{IF}_y(\mathbf{x}_i)$, the influence of a feature \mathbf{x}_i toward y , is measured by the corresponding head degree as

$$\text{IF}_y(\mathbf{x}_i) = d(\mathbf{x}_i) = \sum_{e \in \mathbf{E}} \phi(e) h_{\text{head}}(\mathbf{x}_i, e_{\text{head}}), \quad (9)$$

where $\phi(e)$ denotes the asymmetric interaction contribution along e . h_{head} is defined as

$$h_{\text{head}}(\mathbf{x}_i, e_{\text{head}}) = \begin{cases} 1 & \text{if } \mathbf{x}_i \in e_{\text{head}}, \\ 0 & \text{otherwise.} \end{cases} \quad (10)$$

In the asymmetric interaction graph, the higher the positive $\phi(e)$ of incoming edges, the more positive the influential feature. Conversely, incoming edges with lower negative $\phi(e)$ correspond to the negative influential feature. For example, as shown in Fig.2b, the sum of $\phi(e)$ of incoming edges for "fun" is negative, which is consistent with its negative role in the faithful feature ranking. Generally, for a subset involving the highly influential feature, the interaction contribution is dominated by this feature. While the presence of less influential features do not diminish the asymmetric interaction of other features, their asymmetric interaction contributions tend to be negligible in the presence of influential features.

Given a fixed input instance $\mathbf{x} = (\mathbf{x}_1, \dots, \mathbf{x}_n)$, the contribution of \mathbf{x}_i toward the predicted outcome y could be quantified by the sum of its individual importance and all asymmetric interactions involving \mathbf{x}_i as

$$I(y; \mathbf{x}_i) + \sum_{\substack{T(\mathbf{x}_i) \subseteq n \\ T' \subseteq S \subseteq n \setminus T(\mathbf{x}_i)}} \phi(T' \rightarrow T(\mathbf{x}_i)) + \phi(T(\mathbf{x}_i) \rightarrow T'), \quad (11)$$

where $T(\mathbf{x}_i)$ denotes the subset involving \mathbf{x}_i .

Substituting \mathbf{x}_i with \mathbf{x}'_i resulting an increase or decrease in $f_y(\mathbf{x})$ implies that \mathbf{x}'_i contributes more positively or negatively toward y compared with \mathbf{x}_i . As the presence of less influential features only marginally affect the asymmetric interaction of other features, incorporating \mathbf{x}'_i significantly contributes to

$$I(y; \mathbf{x}'_i) + \sum_{\substack{T(\mathbf{x}'_i) \subseteq n \\ T' \subseteq S \subseteq n \setminus T(\mathbf{x}'_i)}} \phi(T' \rightarrow T(\mathbf{x}'_i)). \quad (12)$$

As discussed in Section 3.2, by substituting "plot" with "script", $f_y(\text{"plot is fun but vague"}) < f_y(\text{"script is fun but vague"})$. Fig.3 demonstrates $I(y; \mathbf{x}_i)$ and pairwise asymmetric interaction $\phi(\mathbf{x}_j \rightarrow \mathbf{x}_i)$. We can observe that compared with "plot", "script" contributes less negatively toward y .

Therefore when computing $f_y(S)$, if the substitute of \mathbf{x}_i substantially influences Eq.(12), $f_y(S)$ will be directional biased toward the predicted outcome y . In computing the Shapley value of faithful influential features with conditional baseline, this directional bias could result in a misinterpretation. As conditional sampling ensures the inherent consistency between features, the replacement of \mathbf{x}_i in $\mathbf{x}_S \cup \mathbf{x}'_{S_2}$ might be (more) influential as \mathbf{x}_i toward y , then $\mathbb{E}(f_y|\mathbf{x}_S \cup \mathbf{x}'_{S_2})$ would be larger than $\mathbb{E}(f_y|\mathbf{x}_{S \cup S_1} \cup \mathbf{x}'_{S_1})$ for ground-positive influential features and smaller for ground-negative influential features. Although increasing sampling size could mitigate these directional biases, it is computationally expensive for high-dimensional instances. Furthermore, larger sample sizes in conditional sampling are not recommended as these baselines ignore inherent feature dependency like random baseline.

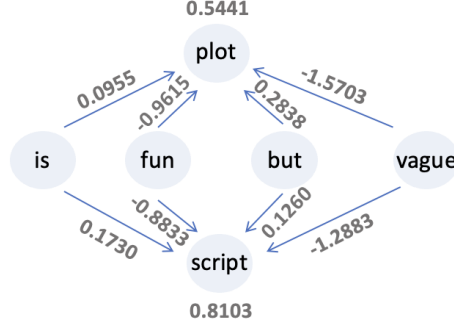


Figure 3: conditional baseline.

4 Proposed method

To mitigate the directional bias toward y generated by the substitute of \mathbf{x}_i (i.e. \mathbf{x}'_i) in $\mathbf{x}_S \cup \mathbf{x}'_{\bar{S}_2}$ and then improve the importance of influential features, we should reduce the contribution of \mathbf{x}'_i to Eq.(12) as

$$\min_{\mathbf{x}'_i \in C} \left| I(y; \mathbf{x}'_i) + \sum_{\substack{T(\mathbf{x}'_i) \subseteq n \\ T' \subseteq S \subseteq n \setminus T(\mathbf{x}'_i)}} \phi(T' \rightarrow T(\mathbf{x}'_i)) \right|, \quad (13)$$

where C denotes the set of possible features of \mathbf{x}'_i to fill in $\mathbf{x}_S \cup \mathbf{x}'_{\bar{S}_2}$.

Based on the triangle inequality (derivation details are provided in Appendix B), the above minimization problem is formulated with

$$\min_{\mathbf{x}'_i \in C} \left| p(y|\mathbf{x}'_i) - p(y) \right| + \sum_{\substack{T(\mathbf{x}'_i) \subseteq n \\ T' \subseteq S \subseteq n \setminus T(\mathbf{x}'_i)}} C_1 \left| \Delta(T', T(\mathbf{x}'_i), \mathbf{x}) \right|, \quad (14)$$

$$\Delta(T', T(\mathbf{x}'_i), \mathbf{x}) = \left| I(y; \mathbf{x}_{T(\mathbf{x}'_i)} | \mathbf{x}_S) - I(y; \mathbf{x}_{T(\mathbf{x}'_i)} | \mathbf{x}_{S \setminus T'}) \right|. \quad (15)$$

For all possible T' , if $I(y; \mathbf{x}_{T(\mathbf{x}'_i)} | \mathbf{x}_S) = I(y; \mathbf{x}_{T(\mathbf{x}'_i)} | \mathbf{x}_{S \setminus T'})$ holds true, it indicates that $T(\mathbf{x}'_i)$ consistently contributes to y across different conditions. In the special case where $\mathbf{x}_{T(\mathbf{x}'_i)}$ is uninformative about y , we will have

$$p(y; \mathbf{x}_{T(\mathbf{x}'_i)} | \mathbf{x}_S) = p(y | \mathbf{x}_S) p(\mathbf{x}_{T(\mathbf{x}'_i)} | \mathbf{x}_S), \quad (16)$$

$$p(y; \mathbf{x}_{T(\mathbf{x}'_i)} | \mathbf{x}_{S \setminus T'}) = p(y | \mathbf{x}_{S \setminus T'}) p(\mathbf{x}_{T(\mathbf{x}'_i)} | \mathbf{x}_{S \setminus T'}), \quad (17)$$

$$I(y; \mathbf{x}_{T(\mathbf{x}'_i)} | \mathbf{x}_S) = I(y; \mathbf{x}_{T(\mathbf{x}'_i)} | \mathbf{x}_{S \setminus T'}) = 0. \quad (18)$$

When considering all possible combinations $\mathbf{x}_{T(\mathbf{x}'_i)}$ involving \mathbf{x}_i , if each combination is uninformative about y , it implies that \mathbf{x}_i does not contribute to y . This is because if \mathbf{x}_i is informative about y , there would be at least some configurations of $\mathbf{x}_{T(\mathbf{x}'_i)}$ contributing to y . Therefore given the special case that can minimize the asymmetric interaction of \mathbf{x}'_i , we conclude that

$$p(y|\mathbf{x}'_i) = p(y), \quad (19)$$

where \mathbf{x}'_i is independent of y .

$p(y|\mathbf{x}'_i) = p(y)$ is the necessary but not sufficient condition for the uninformativeness of $\mathbf{x}_{T(\mathbf{x}'_i)}$ involving \mathbf{x}'_i about y . Therefore $p(y|\mathbf{x}'_i) = p(y)$ leads to minimized $I(y; \mathbf{x}'_i)$ and potentially achieves the special case where the asymmetric interaction involving \mathbf{x}'_i is minimized. Minimizing Eq.(12) is conditionally equivalent⁴ to

$$\begin{aligned} & \min_{\mathbf{x}'_i \in C} \left| I(y; \mathbf{x}'_i) + \sum_{\substack{T(\mathbf{x}'_i) \subseteq n \\ T' \subseteq S \subseteq n \setminus T(\mathbf{x}'_i)}} \phi(T' \rightarrow T(\mathbf{x}'_i)) \right| \\ & \equiv \min_{\mathbf{x}'_i \in C} \left| p(y|\mathbf{x}'_i) - p(y) \right|. \end{aligned} \quad (20)$$

⁴ $p(y|\mathbf{x}'_i) = p(y)$ might not be the only optimal solution.

As $p(y)$ depends on the size and characteristics of the data, we generalize the uninformativeness of \mathbf{x}'_i toward the label space L to avoid estimating $p(y)$ as

$$\max_{\mathbf{x}'_i \in C} - \sum_{j=1}^L p(y_j | \mathbf{x}'_i) \log_2 p(y_j | \mathbf{x}'_i). \quad (21)$$

By maximizing the entropy $H(Y | \mathbf{x}'_i)$, the obtained \mathbf{x}'_i^* is less certain regarding the label space, which is a practical and efficient alternative to minimize the difference between $p(y | \mathbf{x}'_i)$ and $p(y)$.

The greedy search for optimal \mathbf{x}'_i^* in each baseline to compute $\mathbb{E}(f_y | \mathbf{x}_S \cup \mathbf{x}'_{\bar{S}_2})$ is computationally expensive, we design an uncertainty-based reweighting mechanism to accelerate the computation process as

$$\begin{aligned} & \mathbb{E}(f_y | \mathbf{x}_S \cup \mathbf{x}'_{\bar{S}_2}) \\ &= \mathbb{E}_{\mathbf{x}'_{\bar{S}_2}} \left[\hat{H}(\mathbf{x}'_i) \cdot f_y | \mathbf{x}_S \cup \mathbf{x}'_{\bar{S}_2} \right], \end{aligned} \quad (22)$$

where $\hat{H}(\mathbf{x}'_i)$ is the normalized entropy as

$$\hat{H}(\mathbf{x}'_i) = H(\mathbf{x}'_i) / \log_2(L). \quad (23)$$

In the reweighting mechanism higher weight $\hat{H}(\mathbf{x}'_i)$ is assigned to the sequence where \mathbf{x}'_i is less certain toward y and these baselines are encouraged to compute $\mathbb{E}(f_y | \mathbf{x}_S \cup \mathbf{x}'_{\bar{S}_2})$. Furthermore, with flexible generation of $\mathbf{x}'_{\bar{S}_2}$, this reweighting mechanism could be generalized to different baselines, which could improve the faithfulness of feature importance, especially in the scenario where the sampling size is limited. We present the results of applying the uncertainty-based reweighting mechanism to the random and conditional baselines on the motivation example in Fig.1b and it shows that the Shapley interpretations are consistent with the faithful ranking in most cases.

5 Experiments

In this section, we evaluate the faithfulness of Shapley value with and without the uncertainty-based reweighting mechanism. By introducing the reweighting coefficient to the predicting expectation over random baselines (i.e. **random-uw**) and conditional baselines (i.e. **condition-uw**), we compare these Shapley interpretations with the original Shapley values computed by random and conditional baselines (denoted as **random** and **condition**). We adopt Shapley Sampling Štrumbelj and Kononenko [2014] to compute Shapley value (as summarized in Algorithm 1 and 2 in Appendix D).

5.1 Datasets and Models

To effectively leverage language model for conditional sampling, we conduct experiments on various NLP tasks including sentiment analysis (SST-2 Socher et al. [2013] and Yelp-2 Zhang et al. [2015]), natural language inference (SNLI Bowman et al. [2015]), intent detection (SNIPS Coucke et al. [2018]) and topic labeling (20Newsgroup⁵), and study the performance on BERT-base Devlin et al. [2018] and RoBERTa-base Liu et al. [2019] models. Appendix E and F provide the configurations of finetuning pretrained BERT-base and RoBERTa-base models in these downstream tasks.

5.2 Faithful evaluation metrics

We choose three widely used faithful evaluation metrics and employ padding replacement operation. Since deletion-based evaluation yields similar results, we report the corresponding results in Appendix H.

Log-odds (LOR) Shrikumar et al. [2017]: average the difference of negative logarithmic probabilities on the predicted class over the test data before and after replacing the top $k\%$ influential words from the text sequence. The lower LOR, the more faithful feature importance ranking.

Sufficiency (SF) DeYoung et al. [2019]: measure whether important features identified by the explanation method are adequate to remain confidence on the original predictions. The lower SF, the more faithful feature importance ranking.

Comprehensiveness (CM) DeYoung et al. [2019]: evaluate if the features assigned lower weights are unnecessary for the predictions. The higher CM, the more faithful feature importance ranking.

⁵<http://qwone.com/~jason/20Newsgroups/>

5.3 Quantitative Analysis

To alleviate Out-of-Distribution (OOD) issue we choose k within the range $[10, 50]$. The sampling size of computing value function is set to 1000 to enhance the robustness of feature importance ranking. The performance over RoBERTa architecture is reported in Appendix I.

Fig.4 demonstrates the evaluation performance over BERT architecture on different datasets. We can observe that **random-uw** generates more faithful explanations than other baselines. **random-uw** and **condition-uw** always perform better than the corresponding baselines without uncertainty-based reweighting. In SST-2, SNLI and Yelp-2, random-based baselines obtain better results compared with condition-based baselines while for SNIPS and 20Newsgroup **condition-uw** can outperform **random**.

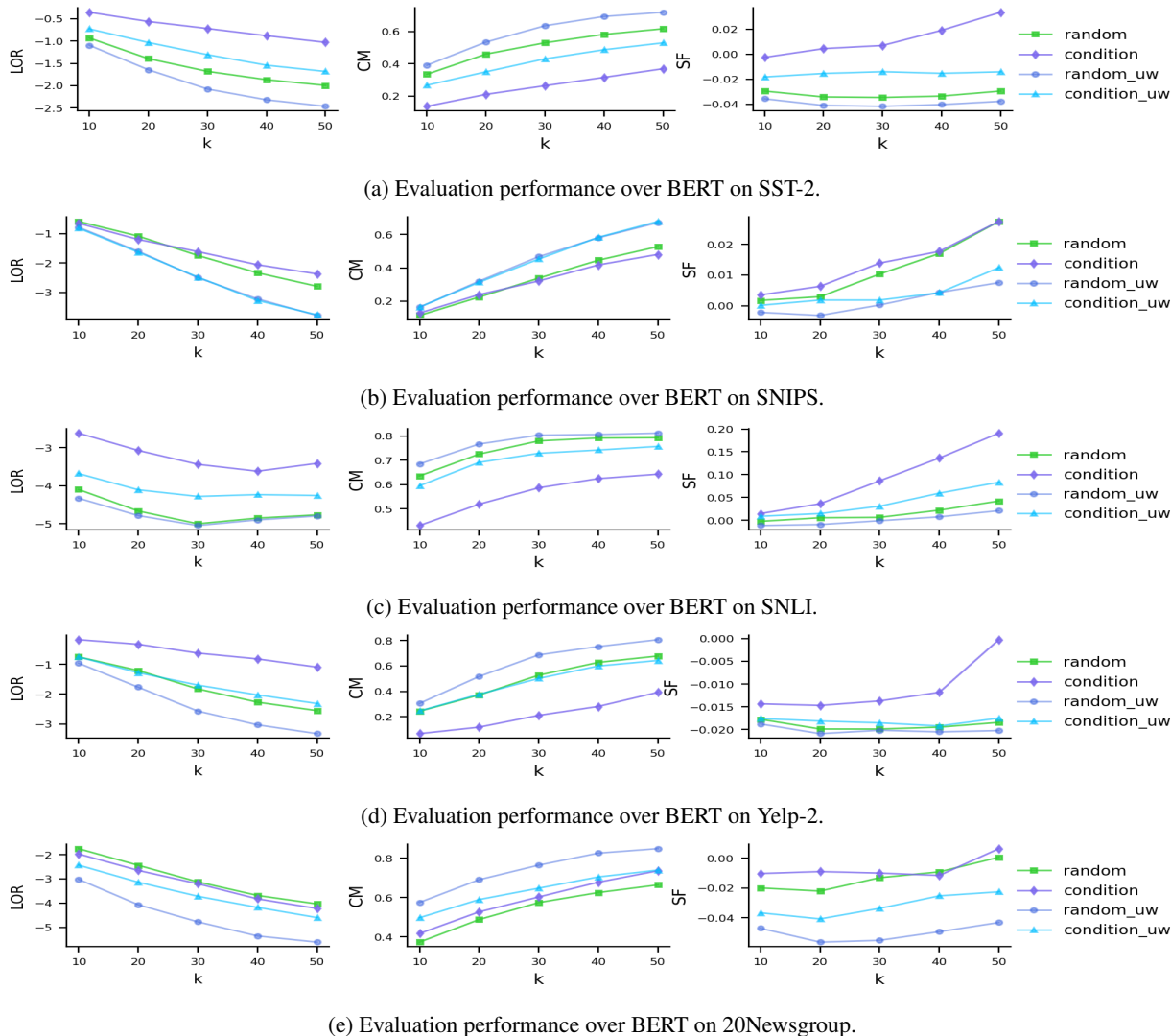


Figure 4: Evaluation performances on the different datasets over BERT architecture.

Based on the above observations, introducing uncertainty-based reweighting to random and conditional baselines can improve the faithfulness of explanations. Furthermore, although random-based baselines are criticized for ignoring feature dependency, these baselines could generate informative local features without introducing additional dependency that tends to result in biased interaction Janzing et al. [2020]. In particular, immediate availability of random baselines can greatly improve the efficiency of Shapley interpretation. We also show the robustness of Shapley Sampling method in Appendix J.

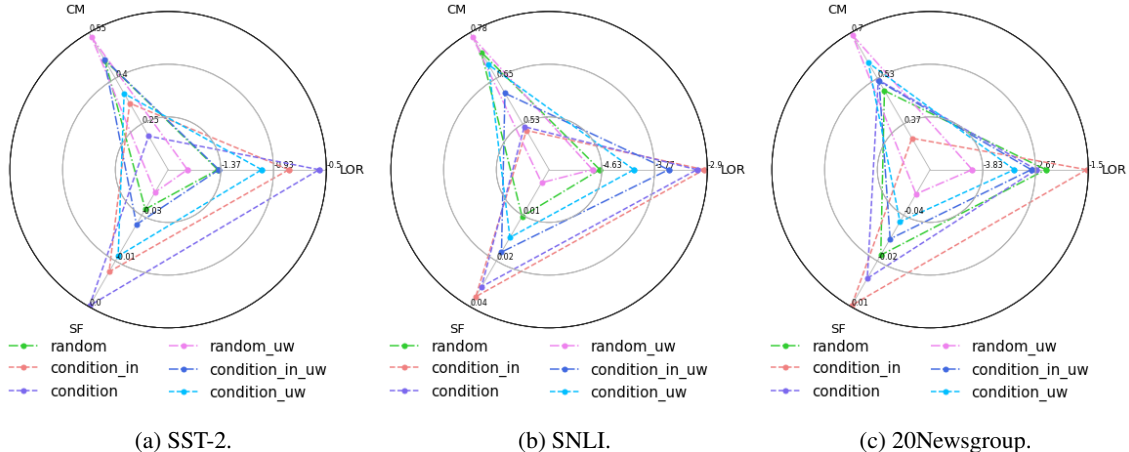


Figure 5: Evaluation performance with $k = 20$ in SST-2, SNLI and 20Newsgroup.

Table 1: Rank correlation coefficient between GPT-4 (or human) and baselines over BERT architecture.

Methods	SST-2		SNIPS	
	GPT-4	Human	GPT-4	Human
random	0.086	0.097	0.175	0.129
condition	0.071	0.115	0.213	0.165
random_uw	0.231	0.229	0.160	0.132
condition_uw	0.161	0.182	0.140	0.095
GPT-4	\	0.710	\	0.856
Human	0.710	\	0.856	\

5.4 Analysis of in-distribution baselines

To address out-of-distribution baselines generated by random sampling or general pretrained language model Kumar et al. [2020], we pretrain BERT-base on these five datasets to ensure in-distribution sampling and evaluate in-distribution baselines (i.e. **condition-in** and **condition-in-uw**) over BERT architecture. Fig.5 shows the evaluation performance with $k = 20$ (the results of Yelp-2 and SNIPS are reported in Appendix K). In-distribution baselines achieve significant improvement over their corresponding baselines without in-distribution sampling. In-distribution sampling does produce in-domain data. However, random sampling from training data also yields in-domain-like data. For example, for the input “most new movies have a bright sheen”, given $x_S =$ “most new movies have”, in-distribution conditional sampling could generate “most new movies have gone the back” and random sampling yields “most new movies have an extraordinary bore” from the sequence “a technical triumph and an extraordinary bore”.

5.5 Human evaluation

There are some research reports Törnberg [2023], Feng et al. [2023] showing that large language models (LLMs), such as GPT-3.5 and GPT-4, can provide high-quality annotations like an excellent crowdsourced annotator does. Therefore we use GPT-4 to provide explanations toward the model’s output (details of the prompt for generating explanation is given in Appendix L). Using the rankings generated by GPT-4 as machine-generated version, we also provide human explanation grounded in human comprehension⁶.

To enable user-friendly human evaluation, we select 83 explained instances for BERT and 74 for RoBERTa on SST-2, and 86 explained instances for both BERT and RoBERTa on SNIPS. First, we employ Spearman’s Rank Correlation Coefficient to measure the correlation of feature importance ranking between GPT-4 (or human) and other baselines, and report the average results in Table 1. It could be observed that GPT-4 and human achieve great consistency, which demonstrates the quality of GPT-4 in human role.

⁶Human evaluation is done by an NLP researcher and we will release these explanations in the public version.

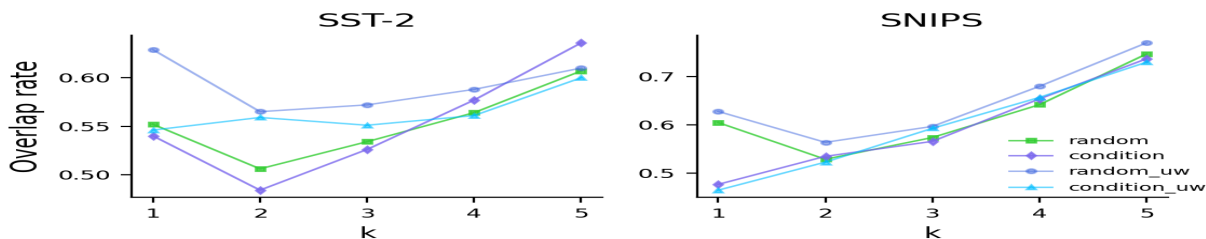


Figure 6: Overlap rate of top $k\%$ influential features between human and baselines over BERT architecture on SST-2 and SNIPS.

Since feature importance ranking between GPT-4 (or human) and other baselines are weakly correlated, we further examine the overlap rate of influential features between GPT-4 (or human) and other baselines. As shown in Fig.6, the overlap rate is always within the range $[45\%, 65\%]$ under smaller k . By conducting quantitative analysis on GPT-4 and human explanations, as shown in Appendix L Fig.13, GPT-4 and human does not perform better than the compared baselines. It should be noted that there still exists a gap between model inference and human understanding Keenan and Sokol [2023].

6 Conclusions

In this paper we analyze the suboptimality of existing random and conditional baselines and identify the problematic baseline where the asymmetric interaction between x'_i (the replacement of the faithful influential feature) and other features has significant directional bias toward the model’s output. We further design a simple uncertainty-based reweighting mechanism to mitigate these biased interactions. By evaluating different baselines on various tasks over BERT and RoBERTa architectures, quantitative analysis shows that our proposed uncertainty-based reweighting mechanism improves the faithfulness of Shapley-based interpretation. We measure the consistency of explanations generated by explainable methods, GPT-4 and human, which demonstrates the gap between model inference and human understanding.

References

- Jacob Devlin, Ming-Wei Chang, Kenton Lee, and Kristina Toutanova. Bert: Pre-training of deep bidirectional transformers for language understanding. *arXiv preprint arXiv:1810.04805*, 2018.
- Aakanksha Chowdhery, Sharan Narang, Jacob Devlin, Maarten Bosma, Gaurav Mishra, Adam Roberts, Paul Barham, Hyung Won Chung, Charles Sutton, Sebastian Gehrmann, et al. Palm: Scaling language modeling with pathways. *arXiv preprint arXiv:2204.02311*, 2022.
- Romal Thoppilan, Daniel De Freitas, Jamie Hall, Noam Shazeer, Apoorv Kulshreshtha, Heng-Tze Cheng, Alicia Jin, Taylor Bos, Leslie Baker, Yu Du, et al. Lamda: Language models for dialog applications. *arXiv preprint arXiv:2201.08239*, 2022.
- OpenAI. Gpt-4 technical report, 2023.
- Been Kim, Martin Wattenberg, Justin Gilmer, Carrie Cai, James Wexler, Fernanda Viegas, et al. Interpretability beyond feature attribution: Quantitative testing with concept activation vectors (tcav). In *International conference on machine learning*, pages 2668–2677. PMLR, 2018.
- Lloyd S Shapley et al. A value for n-person games. 1953.
- Scott M Lundberg and Su-In Lee. A unified approach to interpreting model predictions. *Advances in neural information processing systems*, 30, 2017.
- Jianbo Chen, Le Song, Martin J Wainwright, and Michael I Jordan. L-shapley and c-shapley: Efficient model interpretation for structured data. *arXiv preprint arXiv:1808.02610*, 2018.
- Yongchan Kwon and James Y Zou. Weightedshap: analyzing and improving shapley based feature attributions. *Advances in Neural Information Processing Systems*, 35:34363–34376, 2022.
- Erik Štrumbelj and Igor Kononenko. Explaining prediction models and individual predictions with feature contributions. *Knowledge and information systems*, 41:647–665, 2014.

- Christopher Frye, Damien de Mijolla, Tom Begley, Laurence Cowton, Megan Stanley, and Ilya Feige. Shapley explainability on the data manifold. *arXiv preprint arXiv:2006.01272*, 2020.
- Giles Hooker, Lucas Mentch, and Siyu Zhou. Unrestricted permutation forces extrapolation: variable importance requires at least one more model, or there is no free variable importance. *Statistics and Computing*, 31:1–16, 2021.
- Dominik Janzing, Lenon Minorics, and Patrick Blöbaum. Feature relevance quantification in explainable ai: A causal problem. In *International Conference on artificial intelligence and statistics*, pages 2907–2916. PMLR, 2020.
- I Elizabeth Kumar, Suresh Venkatasubramanian, Carlos Scheidegger, and Sorelle Friedler. Problems with shapley-value-based explanations as feature importance measures. In *International Conference on Machine Learning*, pages 5491–5500. PMLR, 2020.
- David Watson. Rational shapley values. In *2022 ACM Conference on Fairness, Accountability, and Transparency*, pages 1083–1094, 2022.
- Mukund Sundararajan, Ankur Taly, and Qiqi Yan. Axiomatic attribution for deep networks. In *International conference on machine learning*, pages 3319–3328. PMLR, 2017.
- Marco Tulio Ribeiro, Sameer Singh, and Carlos Guestrin. " why should i trust you?" explaining the predictions of any classifier. In *Proceedings of the 22nd ACM SIGKDD international conference on knowledge discovery and data mining*, pages 1135–1144, 2016.
- Pang Wei Koh and Percy Liang. Understanding black-box predictions via influence functions. In *International conference on machine learning*, pages 1885–1894. PMLR, 2017.
- Garima Pruthi, Frederick Liu, Satyen Kale, and Mukund Sundararajan. Estimating training data influence by tracing gradient descent. *Advances in Neural Information Processing Systems*, 33:19920–19930, 2020.
- Michel Grabisch. K-order additive discrete fuzzy measures and their representation. *Fuzzy sets and systems*, 92(2): 167–189, 1997.
- Richard Socher, Alex Perelygin, Jean Wu, Jason Chuang, Christopher D Manning, Andrew Y Ng, and Christopher Potts. Recursive deep models for semantic compositionality over a sentiment treebank. In *Proceedings of the 2013 conference on empirical methods in natural language processing*, pages 1631–1642, 2013.
- Xiang Zhang, Junbo Zhao, and Yann LeCun. Character-level convolutional networks for text classification. *Advances in neural information processing systems*, 28, 2015.
- Samuel R Bowman, Gabor Angeli, Christopher Potts, and Christopher D Manning. A large annotated corpus for learning natural language inference. *arXiv preprint arXiv:1508.05326*, 2015.
- Alice Coucke, Alaa Saade, Adrien Ball, Théodore Bluche, Alexandre Caulier, David Leroy, Clément Doumouro, Thibault Gisselbrecht, Francesco Caltagirone, Thibaut Lavril, et al. Snips voice platform: an embedded spoken language understanding system for private-by-design voice interfaces. *arXiv preprint arXiv:1805.10190*, 2018.
- Yinhan Liu, Myle Ott, Naman Goyal, Jingfei Du, Mandar Joshi, Danqi Chen, Omer Levy, Mike Lewis, Luke Zettlemoyer, and Veselin Stoyanov. Roberta: A robustly optimized bert pretraining approach. *arXiv preprint arXiv:1907.11692*, 2019.
- Avanti Shrikumar, Peyton Greenside, and Anshul Kundaje. Learning important features through propagating activation differences. In *International conference on machine learning*, pages 3145–3153. PMLR, 2017.
- Jay DeYoung, Sarthak Jain, Nazneen Fatema Rajani, Eric Lehman, Caiming Xiong, Richard Socher, and Byron C Wallace. Eraser: A benchmark to evaluate rationalized nlp models. *arXiv preprint arXiv:1911.03429*, 2019.
- Petter Törnberg. Chatgpt-4 outperforms experts and crowd workers in annotating political twitter messages with zero-shot learning. *arXiv preprint arXiv:2304.06588*, 2023.
- Yunhe Feng, Sreecharan Vanam, Manasa Cherukupally, Weijian Zheng, Meikang Qiu, and Haihua Chen. Investigating code generation performance of chatgpt with crowdsourcing social data. In *Proceedings of the 47th IEEE Computer Software and Applications Conference*, pages 1–10, 2023.
- Bernard Keenan and Kacper Sokol. Mind the gap! bridging explainable artificial intelligence and human understanding with luhmann’s functional theory of communication. *arXiv preprint arXiv:2302.03460*, 2023.

A Suboptimal baselines for Shapley value toward the linear model analysis

Consider a simple example $f(x_1, x_2) = x_1 + x_2$ where both X_1 and X_2 follow Bernoulli ($\frac{1}{2}$) and

$$p(x_1, x_2) = \begin{cases} \frac{1}{2} & x_1=x_2, \\ 0 & \text{otherwise.} \end{cases} \quad (24)$$

For linear models, Hooker et al. [2021] shows that permutation-based importance methods associate variable importance with the magnitude of the corresponding coefficient when variable values are standardized. Therefore X_1 and X_2 should be equally informative in permutation-based approaches. Next we will introduce how is the Shapley values computed with different baselines.

Random baseline: $\mathbb{E}(f(x_1, X_2))$ and $\mathbb{E}(f(X_1, x_2))$ is computed as

$$\begin{aligned} \mathbb{E}(f(x_1, X_2)) &= \mathbb{E}_{p(x_2)}(f(x_1, X_2)) \\ &= p(x_2)f(x_1, x_2)|_{x_2=0} + p(x_2)f(x_1, x_2)|_{x_2=1} \\ &= \frac{1}{2}x_1 + \frac{1}{2}(x_1 + 1) \\ &= x_1 + \frac{1}{2}, \end{aligned} \quad (25)$$

$$\begin{aligned} \mathbb{E}(f(X_1, x_2)) &= \mathbb{E}_{p(x_1)}(f(X_1, x_2)) \\ &= p(x_1)f(x_1, x_2)|_{x_1=0} + p(x_1)f(x_1, x_2)|_{x_1=1} \\ &= \frac{1}{2}x_2 + \frac{1}{2}(x_2 + 1) \\ &= x_2 + \frac{1}{2}, \end{aligned} \quad (26)$$

which yields

$$\begin{aligned} \phi_1 &= \frac{1}{2} [v(\emptyset \cup 1) - v(\emptyset) + v(2 \cup 1) - v(2)] \\ &= \frac{1}{2} [\mathbb{E}_{p(x_2)}(f(x_1, X_2)) - \mathbb{E}_{p(x_1, x_2)}(f(X_1, X_2)) + f(x_1, x_2) - \mathbb{E}_{p(x_1)}(f(X_1, x_2))] \\ &= \frac{1}{2} \left[x_1 + \frac{1}{2} - 1 + x_1 + x_2 - x_2 - \frac{1}{2} \right] \\ &= x_1 - \frac{1}{2}, \end{aligned} \quad (27)$$

$$\begin{aligned} \phi_2 &= \frac{1}{2} [v(\emptyset \cup 2) - v(\emptyset) + v(2 \cup 1) - v(1)] \\ &= \frac{1}{2} [\mathbb{E}_{p(x_2)}(f(x_1, X_2)) - \mathbb{E}_{p(x_1, x_2)}(f(X_1, X_2)) + f(x_1, x_2) - \mathbb{E}_{p(x_1)}(f(X_1, x_2))] \\ &= \frac{1}{2} \left[x_2 + \frac{1}{2} - 1 + x_1 + x_2 - x_1 - \frac{1}{2} \right] \\ &= x_2 - \frac{1}{2}, \end{aligned} \quad (28)$$

and $\phi_1 \neq \phi_2$.

Conditional baseline: $\mathbb{E}(f(x_1, X_2))$ and $\mathbb{E}(f(X_1, x_2))$ is computed as

$$\begin{aligned} \mathbb{E}(f(x_1, X_2)) &= \mathbb{E}_{p(x_2|x_1)}(f(x_1, X_2)) \\ &= p(x_2|x_1)f(x_1, x_2)|_{x_2=0} + p(x_2|x_1)f(x_1, x_2)|_{x_2=1} \\ &= 2x_1 \end{aligned} \quad (29)$$

$$\begin{aligned} \mathbb{E}(f(X_1, x_2)) &= \mathbb{E}_{p(x_1|x_2)}(f(X_1, x_2)) \\ &= p(x_1|x_2)f(x_1, x_2)|_{x_2=0} + p(x_1|x_2)f(x_1, x_2)|_{x_2=1} \\ &= 2x_2, \end{aligned} \quad (30)$$

where $p(x_1|x_2) = p(x_2|x_1) = 1$ exclusively when $x_1 = x_2$ and otherwise $p(x_1|x_2) = p(x_2|x_1) = 0$.

Considering two scenarios $x_1 = x_2$ and $x_1 \neq x_2$, we obtain

$$x_1 = x_2, \phi_1 = \phi_2 = \frac{1}{2}(x_1 + x_2 - 1), \quad (31)$$

$$x_1 = 1, x_2 = 0, \phi_1 = \frac{3}{2}, \phi_2 = -\frac{1}{2}, \quad (32)$$

$$x_1 = 0, x_2 = 1, \phi_1 = -\frac{1}{2}, \phi_2 = \frac{3}{2}, \quad (33)$$

therefore with conditional baselines the generated explanations could be misleading.

B Derivation details of Eq.(13)

$$\begin{aligned} & \left| I(y; \mathbf{x}'_i) + \sum_{\substack{T(\mathbf{x}'_i) \subseteq n \\ T' \subseteq S \subseteq n \setminus T(\mathbf{x}'_i)}} \phi(T' \rightarrow T(\mathbf{x}'_i)) \right| \\ & \leq \left| I(y; \mathbf{x}'_i) \right| + \left| \sum_{\substack{T(\mathbf{x}'_i) \subseteq n \\ T' \subseteq S \subseteq n \setminus T(\mathbf{x}'_i)}} \phi(T' \rightarrow T(\mathbf{x}'_i)) \right| \end{aligned} \quad (34)$$

As we focus on the items related to \mathbf{x}'_i , $\left| \sum_{\substack{T(\mathbf{x}'_i) \subseteq n \\ T' \subseteq S \subseteq n \setminus T(\mathbf{x}'_i)}} \phi(T' \rightarrow T(\mathbf{x}'_i)) \right|$ is minimized as

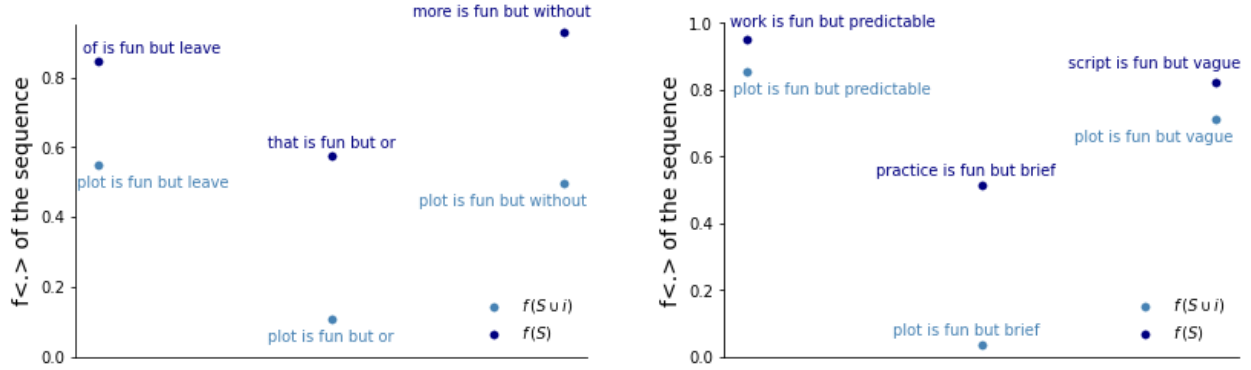
$$\begin{aligned} & \left| \sum_{\substack{T(\mathbf{x}'_i) \subseteq n \\ T' \subseteq S \subseteq n \setminus T(\mathbf{x}'_i)}} \phi(T' \rightarrow T(\mathbf{x}'_i)) \right| \\ & \leq \sum_{\substack{T(\mathbf{x}'_i) \subseteq n \\ T' \subseteq S \subseteq n \setminus T(\mathbf{x}'_i)}} \left| \phi(T' \rightarrow T(\mathbf{x}'_i)) \right| \\ & \leq \sum_{\substack{T(\mathbf{x}'_i) \subseteq n \\ T' \subseteq S \subseteq n \setminus T(\mathbf{x}'_i)}} C_1 \left| \Delta(T', T(\mathbf{x}'_i), \mathbf{x}) \right| \\ & \leq \sum_{\substack{T(\mathbf{x}'_i) \subseteq n \\ T' \subseteq S \subseteq n \setminus T(\mathbf{x}'_i)}} C_1 \left| I(y; \mathbf{x}_{T(\mathbf{x}'_i)} | \mathbf{x}_S) - I(y; \mathbf{x}_{T(\mathbf{x}'_i)} | \mathbf{x}_{S \setminus T'}) \right| \end{aligned} \quad (35)$$

C Demonstrations of the Shapley interpretation for the motivation example

Taking $\mathbf{x}_i = \text{"plot"}$ with $\mathbf{x}_S = \text{"is fun but"}$ as an example, Fig.7 shows some cases where $f_y(S \cup i) < f_y(S)$ with conditional sampling and random sampling.

D Shapley Sampling algorithm

In the Experiment section, we use Shapley Sampling algorithm to estimate Shapley value with random and conditional baselines. The corresponding approximation algorithms are described as follows:



(a) $f_y(S \cup i) < f_y(S)$ with random sampling.

(b) $f_y(S \cup i) < f_y(S)$ with conditional sampling.

Figure 7: The cases where $f_y(S \cup i) < f_y(S)$ with conditional sampling and random sampling.

Algorithm 1 Shapley Sampling algorithm for approximating $\phi(i)$ (**random baseline**).

Input: instance $\mathbf{x} \in \mathcal{X}$, prediction model f , sampling size m
Initialize $\phi(i) = 0$
for 1 **to** m **do**
 randomly select a permutation $\mathcal{O} \in \pi(n)$
 randomly select a instance $\mathbf{x}' \in \mathcal{X}$
 construct two instances:
 $\mathbf{x}_1 \leftarrow \mathbf{x}_{\text{precede } i \text{ in } \mathcal{O}} \cup \mathbf{x}_i \cup \mathbf{x}'_{\text{succeed } i \text{ in } \mathcal{O}}$
 $\mathbf{x}_2 \leftarrow \mathbf{x}_{\text{precede } i \text{ in } \mathcal{O}} \cup \mathbf{x}'_i \cup \mathbf{x}'_{\text{succeed } i \text{ in } \mathcal{O}}$
 if uncertainty-based reweighting **then**
 compute $\hat{H}(\mathbf{x}'_i)$
 $\phi(i) \leftarrow \phi(i) + f_y(\mathbf{x}_1) - \hat{H}(\mathbf{x}'_i) * f_y(\mathbf{x}_2)$
 else
 $\phi(i) \leftarrow \phi(i) + f_y(\mathbf{x}_1) - f_y(\mathbf{x}_2)$
 end if
end for
 $\phi(i) \leftarrow \frac{\phi(i)}{m}$

Algorithm 2 Shapley Sampling algorithm for approximating $\phi(i)$ (**conditional baseline**).

Input: instance $\mathbf{x} \in \mathcal{X}$, prediction model f , sampling size m
Initialize $\phi(i) = 0$
for 1 **to** m **do**
 randomly select a permutation $\mathcal{O} \in \pi(n)$
 construct two instances:
 $\mathbf{x}'_{\text{succeed } i \text{ in } \mathcal{O}} \sim p(\mathbf{x}'_{\text{succeed } i \text{ in } \mathcal{O}} | \mathbf{x}_{\text{precede } i \text{ in } \mathcal{O}} \cup \mathbf{x}_i)$
 $\mathbf{x}_1 \leftarrow \mathbf{x}_{\text{precede } i \text{ in } \mathcal{O}} \cup \mathbf{x}_i \cup \mathbf{x}'_{\text{succeed } i \text{ in } \mathcal{O}}$
 $\mathbf{x}'_{\text{succeed } i \text{ in } \mathcal{O}} \cup \mathbf{x}'_i \sim p(\mathbf{x}'_{\text{succeed } i \text{ in } \mathcal{O}} \cup \mathbf{x}'_i | \mathbf{x}_{\text{precede } i \text{ in } \mathcal{O}})$
 $\mathbf{x}_2 \leftarrow \mathbf{x}_{\text{precede } i \text{ in } \mathcal{O}} \cup \mathbf{x}'_i \cup \mathbf{x}'_{\text{succeed } i \text{ in } \mathcal{O}}$
 if uncertainty-based reweighting **then**
 compute $\hat{H}(\mathbf{x}'_i)$
 $\phi(i) \leftarrow \phi(i) + f_y(\mathbf{x}_1) - \hat{H}(\mathbf{x}'_i) * f_y(\mathbf{x}_2)$
 else
 $\phi(i) \leftarrow \phi(i) + f_y(\mathbf{x}_1) - f_y(\mathbf{x}_2)$
 end if
end for
 $\phi(i) \leftarrow \frac{\phi(i)}{m}$

E Details of the tasks and datasets

Table 2: Summary of the selected datasets (we preprocess the datasets to remove the sequences containing one word and the punctuations at the end of the sequences), where Explained set is randomly sampled from the Test set to avoid high computational complexity and Average sequence length denotes the average sequence length of the instances in Explained set (the length of Yelp-2 explained set is controlled within 50 and we will provide these Explained sets in the public version).

Datasets	Category	Train set	Test set	Explained set	Label set	Average sequence length
SST-2	sentimental analysis	6899	1819	1000	2	19.24
SNIPS	intent detection	13082	700	700	7	9.08
SNLI	natural language inference	54936	7824	1000	3	21.22
Yelp-2	sentimental analysis	559694	37981	200	2	32.12
20Newsgroup	topic labeling	10663	7019	300	20	143.28

F Configurations for finetuning deep models

We use AdamW optimizer with weight decay 0.001 and start with learning rate of $2e-5$ to tune pretrained BERT-base-uncased and RoBERTa-base models. For the setting of epochs and batch size, SST-2 at 10 epochs with a batch size of 32, Yelp-2 also at 10/32, SNLI and SNIPS both at 10/64, and NG at 20/64, ensuring good model performance for each task. The corresponding performance is reported in Table 3.

Table 3: Task performance with finetuning BERT and RoBERTa.

Models	SST-2	Yelp-2	SNLI	SNIPS	20Newsgroup
BERT	90.49	96.20	89.44	97.71	74.48
RoBERTa	94.56	96.87	90.19	97.85	73.37

G Details of the evaluation metrics

Log-odds (LOR) Shrikumar et al. [2017]: average the difference of negative logarithmic probabilities on the predicted class over the test data before and after replacing the top $k\%$ influential words from the text sequence.

$$\text{LOR}(k) = \frac{1}{N} \sum_{i=1}^N \log \frac{f(\mathbf{x}'_i)}{f(\mathbf{x}_i)}, \quad (36)$$

where \mathbf{x}'_i is obtained by replacing the $k\%$ top-scored words from \mathbf{x}_i . The lower LOR, the more faithful feature importance ranking.

Sufficiency (SF) DeYoung et al. [2019]: measure whether important features identified by the explanation method are adequate to remain confidence on the original predictions.

$$\text{SF}(k) = \frac{1}{N} \sum_{i=1}^N f(\mathbf{x}_i) - f(\mathbf{x}_{i,k\%}), \quad (37)$$

where $\mathbf{x}_{i,k\%}$ is obtained by replacing non-top $k\%$ influential elements in \mathbf{x}_i . The lower SF, the more faithful feature importance ranking.

Comprehensiveness (CM) DeYoung et al. [2019]: evaluate if the features assigned lower weights are unnecessary for the predictions.

$$CM(k) = \frac{1}{N} \sum_{i=1}^N f(\mathbf{x}_i) - f(\mathbf{x}_i \setminus \mathbf{x}_{i,k\%}), \quad (38)$$

where $\mathbf{x}_i \setminus \mathbf{x}_{i,k\%}$ is obtained by replacing top $k\%$ influential elements in \mathbf{x}_i . The higher CM, the more faithful feature importance ranking.

H Performance over BERT architecture with deletion operation

Fig.8 demonstrates the evaluation performance over BERT architecture on different datasets with deletion operation. We can observe that **random-uw** outperforms other baselines. **random-uw** and **condition-uw** always perform better than the corresponding baselines without uncertainty-based reweighting. In SST-2, SNLI and Yelp-2, random-based baselines obtain better results compared with condition-based baselines while for SNIPS and 20Newsgroup **condition-uw** can outperform **random**.

I Performance over RoBERTa architecture

Padding and deletion operations generate the same results over RoBERTa architecture. RoBERTa’s training process might make it more robust to variations in input. We can read from Fig.9 that **random-uw** and **condition-uw** achieve comparable performance on SST-2 and SNIPS. Introducing uncertainty-reweighting mechanism can help improve the faithfulness of Shapley explanation.

J Robustness of Shapley Sampling method

We choose smaller sample size 100 with 5 different runs. Table 4, 5 and 6 report the average performance on SST-2, SNIPS and 20Newsgroup over BERT architecture. We can observe that Shapley Sampling method is relatively robust and uncertainty-based reweighting mechanism does increase the performance.

Table 4: Evaluation performance over BERT on SST-2 with $k = 20$.

Methods	SST-2		
	LOR	CM	SF
random	-2.6281±0.0720	0.3884±0.0082	0.0021±0.0010
condition	-2.2590±0.0608	0.3515±0.0082	0.0272±0.0020
random_uw	-3.9181±0.0661	0.5533±0.0067	-0.0090±0.0010
condition_uw	-3.1907±0.0600	0.4635±0.0065	0.0014±0.0031

Table 5: Evaluation performance over BERT on SNIPS with $k = 20$.

Methods	SNIPS		
	LOR	CM	SF
random	-1.1928±0.0369	0.2436±0.0065	0.0029±0.0023
condition	-1.1288±0.0432	0.2322±0.0074	0.0061±0.0008
random_uw	-1.7017±0.0447	0.3317±0.0074	-0.002±0.0015
condition_uw	-1.5808±0.0301	0.3100±0.0060	0.0008±0.0014

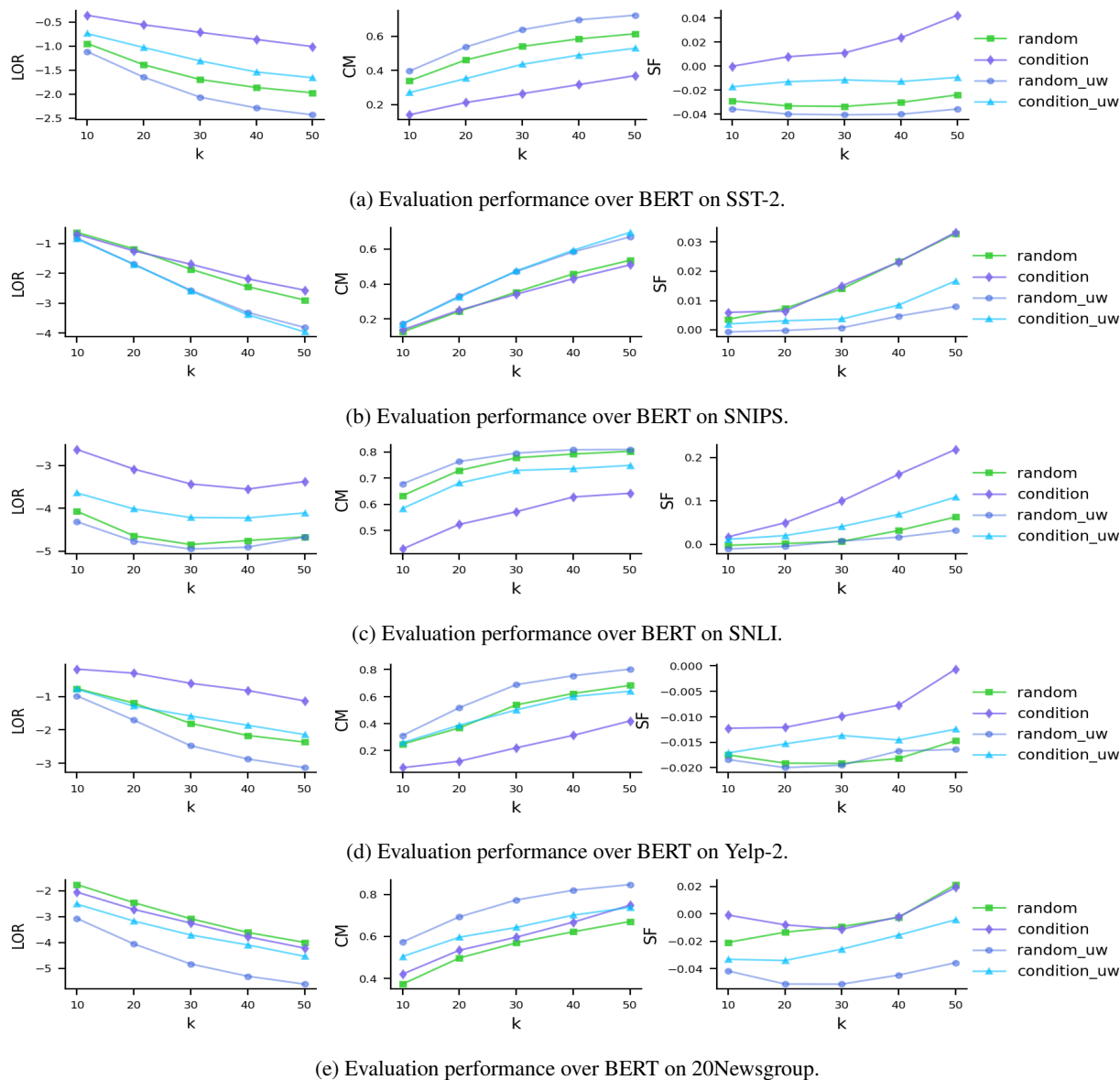
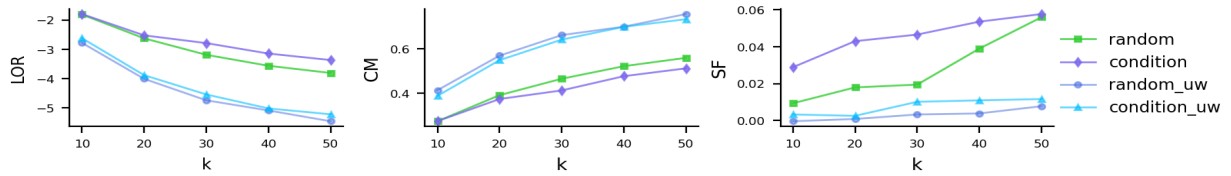


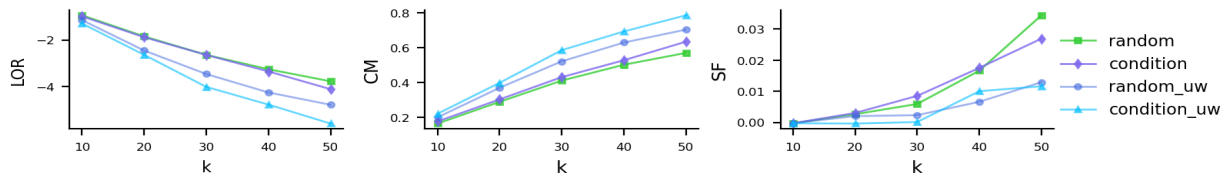
Figure 8: Evaluation performances on the different datasets over BERT architecture.

Table 6: Evaluation performance over BERT on 20Newsgroup with $k = 20$.

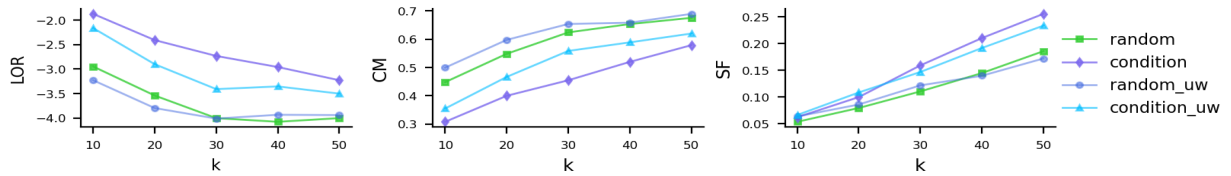
Methods	20Newsgroup		
	LOR	CM	SF
random	-2.4960 ± 0.0638	0.4706 ± 0.0062	-0.0258 ± 0.0048
condition	-2.7000 ± 0.1045	0.5301 ± 0.0181	-0.0186 ± 0.0076
random_uw	-4.1049 ± 0.0646	0.7014 ± 0.0118	-0.0567 ± 0.0032
condition_uw	-3.2504 ± 0.0852	0.5952 ± 0.0152	-0.0356 ± 0.0046



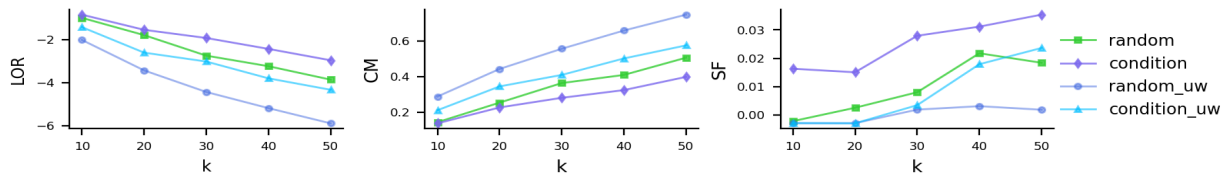
(a) Evaluation performance over RoBERTa on SST-2.



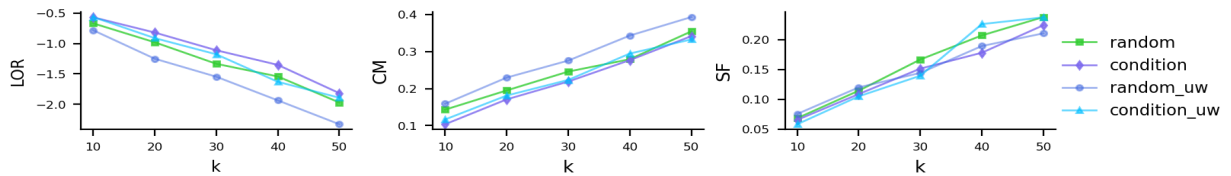
(b) Evaluation performance over RoBERTa on SNIPS.



(c) Evaluation performance over RoBERTa on SNLI.



(d) Evaluation performance over RoBERTa on Yelp-2.



(e) Evaluation performance over RoBERTa on 20Newsgroup.

Figure 9: Evaluation performances on the different datasets over RoBERTa architecture.

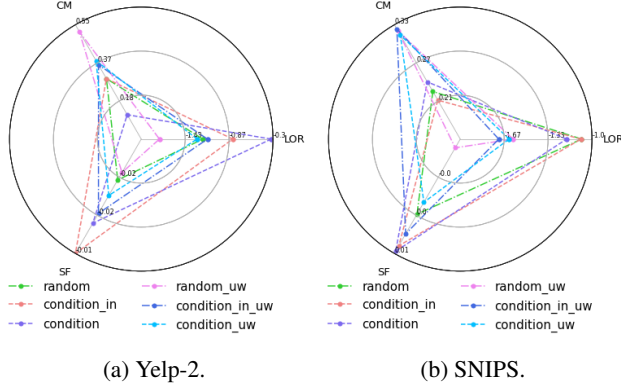


Figure 10: Evaluation performance with $k = 20$ in Yelp-2 and SNIPS.

Table 7: Illustration of how to use GPT-4 to generate explanations. “Input” and “Output” refer to the prompt provided to GPT-4 and the generated explanations, respectively. It could be treated as zero-shot evaluation. We maintained the output integrity without alternations, while occasionally adjusting the requirements to ensure a complete ranking. For instance, when dealing with repeated strings, each instance was assigned an individual rank.

Component	Description
Input	<p>The task is described as follows: given a text sequence of a movie review with the sentiment classification label (positive or negative), there are a few requirements:</p> <ol style="list-style-type: none"> 1. Transform this long string sequence into a list of strings (denoted as a transformed list). 2. Measure the contributions of each string in the list toward the sentiment label based on your understanding. Then rank all strings (ensuring that no strings are excluded) including the repeated strings (each occurrence should have its own rank) in this list based on their contributions. 3. The ranking should follow an order from the most positive to neutral to the most negative. Place the strings with the highest positive contribution at the top and the strings with the most negative contribution at the bottom. 4. Output all ranked strings ensuring that no strings are excluded.
Example Input	<p>Sequence: something the true film buff will enjoy Label: positive</p>
Example Output	<p>Transformed list: ['something', 'the', 'true', 'film', 'buff', 'will', 'enjoy'] Ranked strings: ['enjoy', 'true', 'something', 'film', 'buff', 'will', 'the']</p>

K In-distribution baselines

Fig.10 shows the evaluation performance with $k = 20$ on Yelp-2 and SNIPS. Similarly, in-distribution baselines outperforms their corresponding baselines without in-distribution sampling.

L Human evaluation

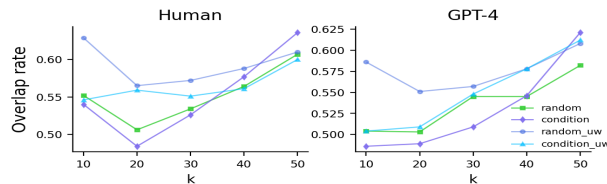
Table 7 demonstrates how to use GPT-4 to generate explanations and Table 8 shows an example of explanations generated by different baselines, GPT-4 and human over BERT architecture. Table 9 and Fig.12 shows that the explanations provided by GPT-4 (or human) are not closely correlated with the explanation generated by different baselines. Fig.13 reports the quantitative analysis of explanations provided by GPT-4 and human.

Table 8: An example of explanations provided by different baselines, GPT-4 and human over BERT architecture.

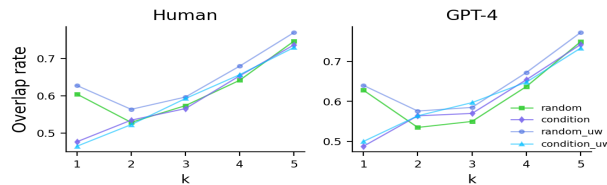
Methods	sequence: most new movies have a bright sheen label: positive
random	'bright', 'sheen', 'have', 'new', 'a', 'movies', 'most'
condition	'bright', 'movies', 'new', 'most', 'have', 'sheen', 'a'
random_uw	'bright', 'sheen', 'have', 'new', 'a', 'movies', 'most'
condition_uw	'bright', 'movies', 'new', 'most', 'sheen', 'have', 'a'
GPT-4	'bright', 'sheen', 'most', 'new', 'movies', 'have', 'a'
Human	'bright', 'sheen', 'most', 'new', 'movies', 'have', 'a'

Table 9: Rank correlation coefficient between GPT-4 (or human) and baselines over RoBERTa architecture.

Methods	SST-2		SNIPS	
	GPT-4	Human	GPT-4	Human
random	0.033	0.095	0.186	0.129
condition	0.142	0.173	0.050	-0.001
random_uw	0.152	0.113	0.189	0.121
condition_uw	0.203	0.137	0.094	0.038
GPT-4	\	0.772	\	0.830
Human	0.772	\	0.830	\



(a) SST-2.



(b) SNIPS.

Figure 11: Overlap rate of top k influential features between GPT-4 (or human) and baselines over BERT architecture on SNIPS.

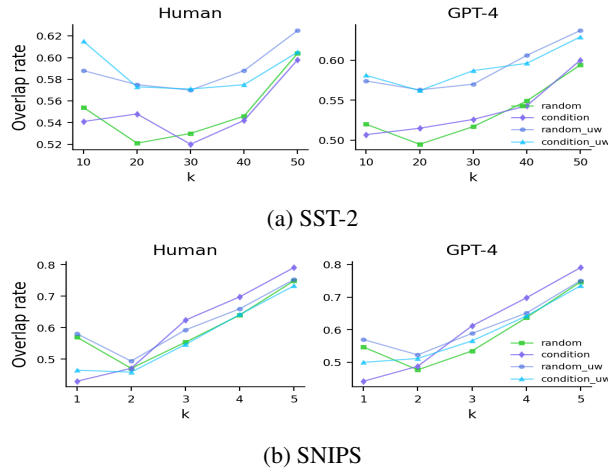


Figure 12: Overlap rate of top influential features between GPT-4 (or human) and baselines over RoBERTa architecture in SST-2 and SNIPS.

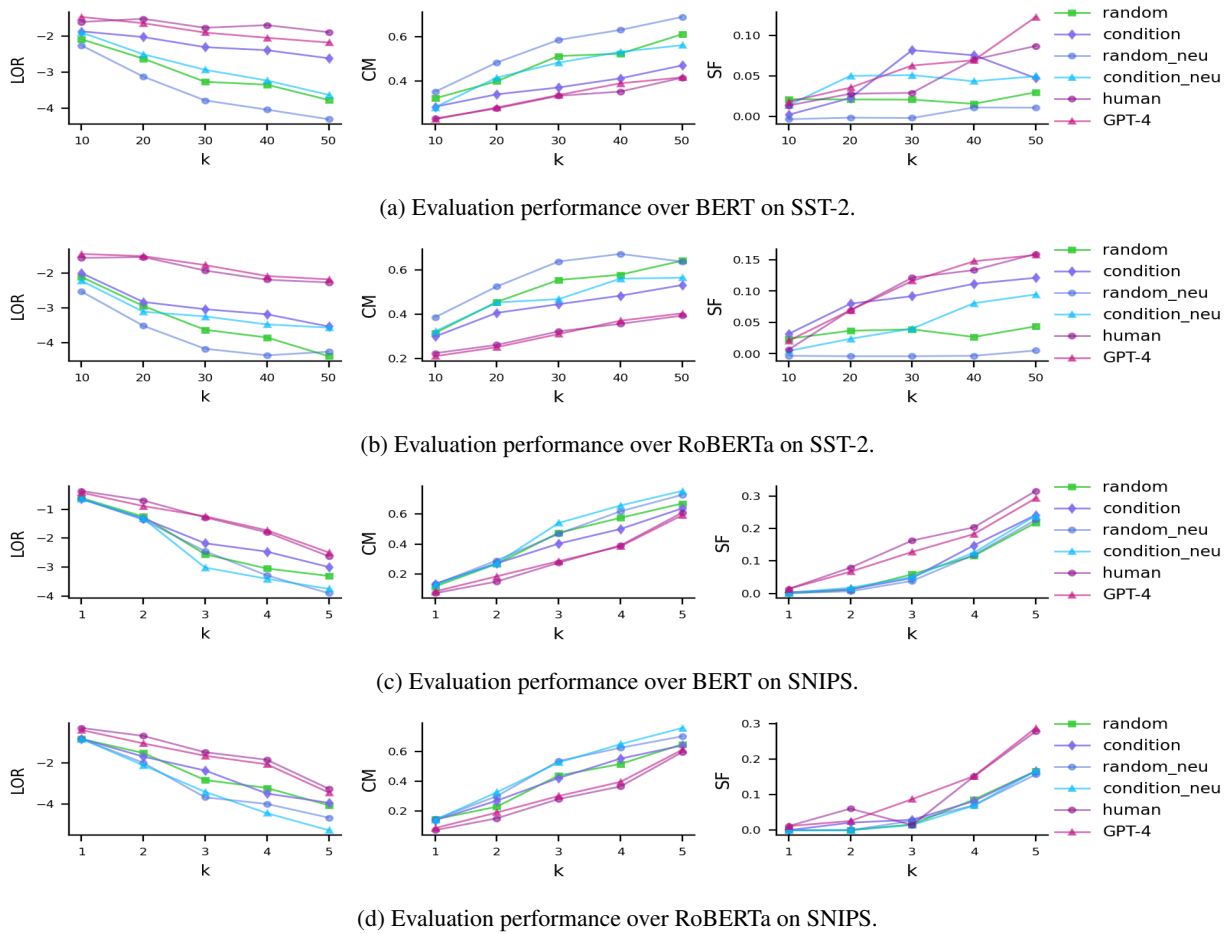


Figure 13: Evaluation performances on SST-2 and SNIPS.